Letters in Applied NanoBioScience
Open-Access Journal (ISSN: 2284-6808)

Article
Volume 13, Issue 4, 2024, 172
https://doi.org/10.33263/LIANBS134.172

Antimicrobial Efficacy of Oil-in-Water Nanoemulsion Against *Vibrio fluvialis* and *Vibrio mimicus*

Jahangir Ahmed [1], Nafeela Hauva N [1], Karthikeyan Ramalingam [1,*]

[1] School of Life Sciences, B.S. Abdur Rahman Crescent Institute of Science and Technology, Chennai, Tamil Nadu- India
* Correspondence: karthikeyan.sls@crescent.education (K.R.);

Scopus Author ID 57909451000
Received: 31.08.2023; Accepted: 12.05.2024; Published: 27.08.2024

Abstract: The study focuses on assessing the antimicrobial properties of a nanoemulsion against *Vibrio spp.,* including *Vibrio fluvialis* and *Vibrio mimicus*, which are known to cause diseases in aquaculture. It has been periodically inducing gastroenteritis by transmitting various diseases to humans and causing illness. The castor and olive oil nanoemulsions (CA-NE and OL-NE) were prepared using micro-fluidization techniques and characterized by DLS to determine the size, zeta potential, and polydispersity index. The effectiveness of the nanoemulsion was evaluated against pathogenic *Vibrio spp*. by preliminary tests such as minimum inhibitory concentration and minimum bactericidal concentration using the microdilution method. Additional tests included adherence, antibiofilm assays, live/dead staining, and oxygen consumption rate (OCR) studies. The anti-adherence efficacy for OL-NE was 45.33% against *V. fluvialis*, whereas gentamicin exhibited an inhibition rate of 29.27%. In the biofilm assay, OL-NE showed higher inhibition, achieving rates of 45.89%, against *V. fluvialis*. The live/dead staining results indicated that OL-NE caused a significant percentage of dead cells (54.72%) against the *V. mimicus*, comparable to the current antibiotic gentamicin (54.87%). The oxygraph analysis measured the oxygen consumption rate (OCR) of CA-NE showed a reduction of 0.67, while the current antibiotics exhibited a 0.89-fold reduction against *V. fluvialis*. This indicates that CA-NE had a better reduction rate (0.22-fold) than the current antibiotics compared to untreated (1.0). Thus, nanoemulsions have better results observed with adherence, biofilm, and OCR rate against *V. fluvialis*, whereas live/dead results are better against *V. mimicus.* Notably, in all cases, NEs surpassed the performance of the current antibiotics and exhibited a successful inhibition rate.

Keywords: *Vibrio Spp*; *Vibrio fluvialis*; *Vibrio mimicus*; nanoemulsion; aquaculture.

1. Introduction

Vibrio mimicus and *Vibrio fluvialis* are halophilic Gram-negative bacterium, emerging pathogens predominantly found in aquatic environments. These share a close relationship with *V. cholerae* and are known to induce gastroenteritis. This condition is characterized by diarrhea, nausea, vomiting, abdominal pain, and fever. The primary cause of infection is the consumption of contaminated seafood [1,2]. The specific mechanisms underlying the pathogenicity of *V. mimicus* remain unknown. However, studies have indicated that *V. mimicus* can produce multiple virulence factors, adhesins, hemolysins, various proteases such as collagenases and metalloproteases, siderophores, cytolysins, lipases, and DNases [3,4]. The *V. mimicus* bacterium synthesizes a cytolytic/hemolytic toxin known as *V. mimicus* hemolysin (VMH). The vmhA gene encodes this heat-labile toxin and can be found in both environmental

and clinical strains of *V. mimicus* [5-7]. Studies have indicated that *V. mimicus* exhibits certain genotypic similarities to *V. cholerae*, including the presence of the ctxA/B operon. This operon encodes the cholera toxin, whose gene is typically found in the genome of the bacteriophage CTXΦ, known to infect *V. cholerae*. These findings suggest the occurrence of horizontal transfer of this phage between *V. cholerae* and *V. mimicus* [7,8].

Meanwhile, the infection caused by *V. fluvialis* is primarily associated with sporadic cases and outbreaks of gastroenteritis characterized by cholera-like diarrhea. While uncommon, *V. fluvialis* can potentially cause extraintestinal infections, such as hemorrhagic cellulitis with cerebritis, bacteremia, peritonitis, acute otitis, and endophthalmitis [9-15]. The exact route by which *V. fluvialis* enters the biliary system is unknown. However, it is hypothesized that entry may occur through a cutaneous lesion or via gastrointestinal translocation following consuming contaminated seafood, similar to observations made in other *Vibrio infections* [16,17]. Multiple reports have reported infections caused by *V. mimicus* and *V. fluvialis* in various countries, indicating that certain strains possess genes capable of causing illness by consuming raw or undercooked seafood products [18-20]. However, there is a lack of studies investigating the control and cure of these pathogenic strains. In our research, nanoemulsions have therapeutic potential by conducting various tests against both *V. mimicus* and *V. fluvialis* obtained from microbial types of culture collection (MTCC).

Nanoemulsions are complex systems comprising two immiscible liquids, where one liquid phase is dispersed as tiny droplets within a continuous liquid phase. These droplets, typically ranging in size from 20 to 1000 nm, are stabilized by suitable surfactant and cosurfactant. Specifically, Oil-in-Water (O/W) nanoemulsions, widely used in food delivery systems, consist of oil droplets dispersed within an aqueous medium. These nanoemulsions employ surfactants approved for human consumption and are commonly found in food substances classified as Generally Recognized as Safe (GRAS) by the FDA [20-23]. Our NEs are prepared by micro-fluidization method using various edible oils, such as castor and olive oil. We analyzed the killing effects of planktonic and the biofilm form of *V. mimicus* and *V. fluvialis*, including the positive control (Gentamicin) and growth control. Additionally, the antimicrobial effects of a nanoemulsion will be examined by conducting various tests such as MIC, MBC, anti-adherence, biofilm, live/dead, and oxygen consumption rate studies.

2. Materials and Methods

2.1. Bacterial strains and growth conditions.

The *V. fluvialis* (MTCC-4432) and *V. mimicus* (MTCC-4434) were obtained from the Microbial Type Culture Collection (MTCC) in Chandigarh, India. The castor and olive oil (SF) were acquired from the local market in Tambaram, Tamil Nadu. The surfactant used Polysorbate 60 (Tween 60), and the co-surfactants cetylpyridinium chloride, agar, and tryptose soya broth (TSB) were obtained from HI-media and Sisco Research Laboratories (SRL) in Mumbai, India. The bacterial cultures were stored at -80°C in TSB supplemented with 50% (v/v) glycerol. Stock mother cultures were inoculated and cultured at 37°C in fresh sterile broths containing 1.5% NaCl. Fresh inoculums were used for each experiment, and the bacterial density was determined by measuring the optical density at 600 nm, corresponding to approximately 10^7 CFU/mL.

2.2. Nanoemulsions production and characterizations.

The process and procedure for NE followed earlier studies with modifications [24]. The processing of two nanoemulsions (NEs) oil-in-water (O/W) combinations was prepared. The combinations utilized a nanoemulsion composition consisting of castor and olive oil (25%) with Tween-60 (2.5%) as surfactant and cetylpyridinium chloride (CPC-1%) as co-surfactant.

The Microfluidizer-LM10, manufactured by (Microfluidics Int. Corporation in the USA), was employed to achieve emulsification. The NE solutions were thoroughly mixed using a magnetic stirrer and then subjected to emulsification at 20,000 psi/lb/in2, repeated three times at room temperature. The prepared nanoemulsion was also characterized by dynamic light scattering (Malvern Zeta-sizer Nano ZSP instrument) for size and zeta potential determinations.

2.3. MIC and MBC of Vibrio pathogens.

The antibacterial activity of castor and olive oil NEs (CA-NE and OL-NE) was evaluated by determining their MIC and MBC values. In most cases, MBC concentrations were found to be greater than MIC. The bacteriostatic and bactericidal methodology was used in a microtiter (96-well plate) to examine the antibacterial capabilities of generated nanoemulsions against *V. fluvialis* and *V. mimicus* pathogenic strains using the micro-dilution method [25]. The 100 µl of (2x) TS-broth and 100 µl of NEs from each group were added to the initial well and orderly diluted up to the 12th well. This experiment used sterile ultrapure water (UPH2O) containing medium without bacteria, a positive control gentamicin, as a negative control. After inoculating each well with 5 µl of a standardized cell suspension containing CFU/ml, the plates were placed in an incubator at 37°C overnight. The MIC is the lowest concentration of the test substance, which inhibits visual bacterial growth. At the same time, the MBC is the lowest concentration, which leads to the absence of any observable growth on agar (99.9% mortality). For maximum bactericidal concentration (MBC) testing, aliquots of test wells containing no visual growth were inoculated onto TS-agar and subjected to an additional overnight incubation at 37°C. The MBC was documented as having occurred at the most significant dilution, where there were no survivors of the bacterial populations [26,27].

2.4. Adherence potential of nanoemulsions.

The adherence potential of our nanoemulsion optimized concentration was applied to 5 ml test tubes containing bacterial cultures containing 10^7 CFU/ml overnight, followed by earlier studies [27]. Therefore, during 24h, the tubes were placed at a 30-degree angle and incubated at 37°C overnight to measure the adherence potential of nanoemulsions. The methanol was used to fix the developed bacteria adherence on the surface of the test tubes for 15 min. After that, we emptied the tubes and let them air dry. Additionally, 5 ml of crystal violet solution (1% v/v) was added to each test tube and allowed to sit for 5 min. Putting the tube under running water helped remove any remaining color stain. After letting the microplates air dry, 5 ml of 33% (v/v) glacial acetic acid was used in each test tube to dissolve the bacteria attached to the adhering cells. Each experiment was performed in three independent sets for each repeat to conclude the results. The bound bacteria's solution was measured using a Multilabel-detector (Perkin Elmer) at 590 nm. As a reference point, the optical densities of each set of samples were adjusted by subtracting the values for the growth control.

2.5. Biofilm quantification.

The following procedure was followed to develop biofilms on microtiter plates (96 well plates) and treat them with nanoemulsion [28]. Initially, 10 µl of an overnight broth culture was added to each well. The plate was then incubated aerobically at 37°C for 72 hours. At 12-hour intervals, the medium containing the suspended bacteria was discarded and replaced with an equal volume of fresh medium. This step ensured the maintenance of optimal growth conditions. Negative controls were established by incubating microplates with medium, without bacterial inoculation. Next, the supernatant medium was removed, and the biofilms were treated with different optimized volumes of selected nanoemulsion. The emulsion was applied to the biofilms for 1hrs at room temperature without agitation. Subsequently, the wells were rinsed twice with distilled water to remove any remaining traces of the emulsion. Plastic microtiter plates were utilized to measure biofilm viability. The methanol was added to each well and left for 15 minutes to fix the attached bacteria. The microplates were then emptied and allowed to air dry. Each well was stained with 1% (v/v) of crystal violet solution for 5 minutes. After staining, the microplates were washed to eliminate the excess stain and again allowed to air dry. To remove the dye from the adhering cells, 33% (v/v) glacial acetic acid was added to each well. Using a microplate reader, the resultant solutions were measured for optical density at 590 nm. The optical densities of each sample set were adjusted by subtracting the values obtained for the growth control. Each control was repeated thrice to ensure the experiment's reliability.

2.6. Live/dead assay.

Biofilm viability was evaluated by cultivating *V. fluvialis* and *V. mimicus* in TS broth with 1.5% NaCl for 72 h on 24-well plates. The grown biofilm was treated with NE for 1h. After that, we thoroughly rinsed the wells with distilled water twice to ensure we got every last bit of that emulsion. After 15 min, the adhering bacteria were fixed by adding 2.5 ml of methanol to each well. The microplates were left to air dry after being emptied. Afterward, we stained each well for 5 min with 2.5 ml of crystal violet 1% (v/v). Any leftover stain on the microtiter was washed away. After letting the microplates air dry, we added 2.5 ml of 33% (v/v) glacial acetic acid to each well to dissolve the dye from the adhering cells. The biofilm was stained with a LIVE/DEAD^{TM} BacLight^{TM} [29] Bacterial Viability Kit from Invitrogen (Thermofisher Scientific) and was used to dye the biofilm after treatment. Before use, the live/dead stain was brought to room temperature from its storage temperature of -20°C. SYTO-9 was combined (.1µl)/well for staining, which was then allowed to stand the wells for 15 min [30]. The samples were checked immediately using a 490 nm wavelength. The untreated bacterial cells in the untreated wells were designated as controls and counted to remove the absorbance readings of live and dead cells. For each experimental condition, three separate experiments were conducted.

2.7. Oxygen consumption rate study of nanoemulsions.

The Clarke electrode-based Oxygraph instrument (Hansatech, Norfolk, UK) was used to measure oxygen consumption rates (OCR) in accordance with the manufacturer's instructions [31,32]. About 1×10^7 cells suspended in fresh TS-broth during the exponential phase, with or without the test compounds, were used. With the help of the O_2 View program

version 2.0, the findings were analyzed, and the rates were expressed as nanomoles of oxygen consumed by 1×10^7 cells/milliliter/minute.

3. Results and Discussion

3.1. Size and zeta potential analysis of nanoemulsion.

The nanoemulsions were subjected to emulsification using a microfluidizer, and their size and zeta potential were subsequently determined using a DLS (Malvern Zeta-sizer Nano ZSP instrument) [33]. The synthesized nanoemulsions were further characterized, leading to the following observations: CA-NE had an average particle size of 229.7 nm zeta potential of 41.8mV, and a polydispersity index (PDI) was measured to be 0.108 (Figure 1A). OL-NE exhibited an average particle size of 190.2 nm, a zeta potential of 49.1 mV, and a polydispersity index of 0.251 (Figure 1B). These measurements provide valuable information about the physical properties of the nanoemulsions. Notably, CA-NE had a larger particle size compared to OL-NE, which conformed to DLS. The zeta potential values also indicated that all the nanoemulsion particles carried a net positive charge. This characterization data plays a crucial role in understanding the stability and potential applications of the synthesized nanoemulsions [34].

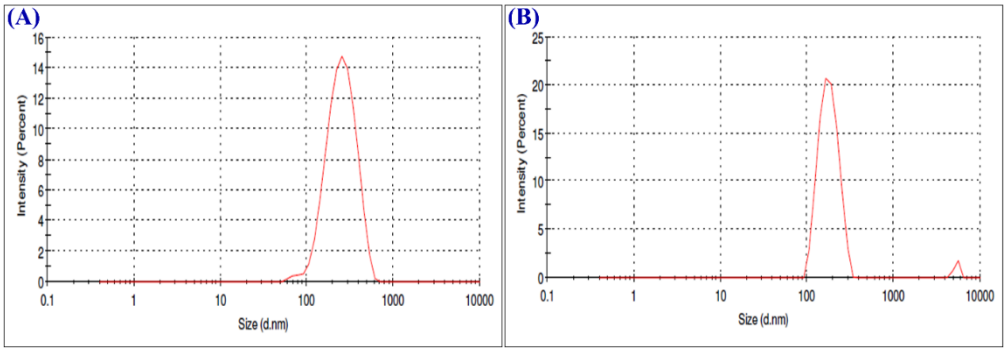

Figure 1. The mean droplet size distribution and zeta potential of castor and olive oil nanoemulsions were measured as **(A)** CA-NE; and **(B)** OL-NE. These nanoemulsions were generated through three emulsification processes, each conducted at a pressure of 20,000 lb/in² using a microfluidizer (LM-10).

3.2. MIC and MBC test results.

The minimum inhibitory concentration (MIC) represents the lowest concentration of an antimicrobial agent required to eliminate a microorganism. Regarding efficacy, higher MIC dilutions (D) were observed for OL-NE (1-128 and 1-256) as comparable. Similarly, the minimum bactericidal concentration (MBC) and the sub-culture on Ts-agar media showed promising results for CA-NE and OL-NE (2-64 and 2-128 dilutions) as well as the antibiotic gentamicin (MIC-1-512 and MBC-2-256; 80 mg/2ml concentrations) against the *V. fluvialis* (MTCC-4432) (Figure 2A). Similarly, against the *V. mimicus* (MTCC-4434), the MIC dilutions for CA-NE and OL-NE were noted as 1-64 and 1-256, respectively. The MBC was effective at a dilution of 2-32 and 2-128 (Figure 2B). In contrast, antibiotics are (1-64 and 2-32), respectively. Food-borne pathogens from the aquaculture environment, virulence assessment, genetic diversity, and antimicrobial resistance are necessary for developing preventive strategies and combating the spread. This resistance could be attributed to virulent gene mutations and other causes of excessive use of antibiotics to control bacterial infectious diseases [35,36]. In summary, nanoemulsions such as OL-NE exhibited considerable effectiveness against both strains, especially at higher dilution rates. So, the nanoemulsion

could be used as an alternative to current antibiotics to control the spread of such pathogens' disease.

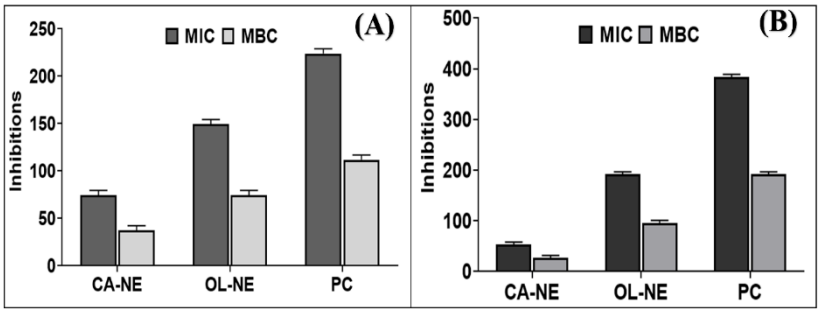

Figure 2. The antibacterial efficacy of castor and olive oils nanoemulsion was tested against pathogenic strains of *V. fluvialis* and *V. mimicus* by employing micro-dilutions. The commercially purchased **(A)** *V. fluvialis*; **(B)** *V. mimicus*. CA-NE-Castor Oil-Nanoemulsion, OL-NE-Olive Oil-Nanoemulsion; MIC-minimum inhibitory concentration; MBC-minimum bactericidal concentration; PC (positive control).

3.3. Anti-adherence potential of nanoemulsions.

In this study, the effectuality of the castor and olive oil nanoemulsions was checked in both strains, and the effectuality was assessed using the test-tube adherence inhibition method. The results emphasize bacterial adhesins' crucial role in hosts' pathogenicity, making them a promising target for developing innovative antibacterial techniques [26,36]. Furthermore, the inhibitory effects of castor and olive oil nanoemulsions on *V. fluvialis and V. mimicus* were evaluated and compared to the antibiotic gentamicin (Ab). Both the nanoemulsions exhibited inhibition against *V. fluvialis and mimicus*. NE demonstrated significantly higher levels of inhibition compared to current antibiotics reported against *V. fluvialis*, with rates of CA-NE at 16.94% and OL-NE at 45.33%, among which OL-NE was better than the antibiotic's inhibition rate of 29.27% (Figure 3A).

In contrast, for the *V mimicus*, the inhibition was reported at CA-NE and OL-NE at 44.61% and 24.53%, whereas the antibiotics reduction rate was 24.15% (Figure 3B). CA-NE displayed significantly higher comparable inhibition compared to current antibiotics. The earlier study raises awareness of antibiotic-resistant *Vibrio* species in intensive shrimp farming systems, contributing to strategies for reducing *Vibrio* antibiotic resistance in aquaculture [27]. The NEs anti-adhesion mechanism may provide an entirely novel method for controlling *V. fluvialis* and *V. mimicus* colonization in the host and interrupting the first stage of infection, which may prevent disease transfer.

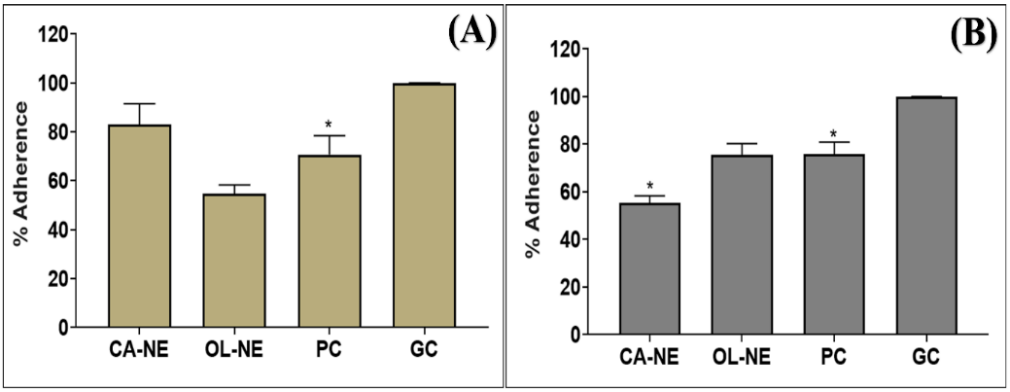

Figure 3. Evaluation of adhesion potential of nanoemulsions containing castor and olive Oil against **(A)** *V. fluvialis*; **(B)** *V. mimicus* Strains. CA-NE-Castor Oil-Nanoemulsion, OL-NE Olive-Oil-Nanoemulsion, PC (Positive Control-Gentamicin); GC (Growth control).

3.4. Biofilm quantification assay.

A biofilm assay can be performed to study biofilm formation. The standard method used a microtiter plate, where bacterial cells are grown, and their ability to form biofilms is assessed. Two nanoemulsions were tested, mainly CA-NE and OL-NE, as inhibition was noted at 39.29% and 45.89%. OL-NE demonstrated a high level of inhibition when compared to the current antibiotic gentamicin at 43.31%, as shown in (Figure 4A) against commercial *V. fluvialis* (MTCC-4432). At the same time, *V. mimicus* (MTCC-4434) was tested, and inhibition potential was observed in CA-NE at 33.78%, OL-NE at 38.58%, and with antibiotics (gentamicin) at 38.0%, shown in (Figure 4B). Higher eradication potential was noted in OL-NE combinations. The assay is used to measure the effectiveness of different aspects of biofilm formation, such as the amount of biomass or the thickness of the biofilm. According to an earlier study, all tested nanoemulsions demonstrated good inhibition against multi-drug-resistant ESKAPE pathogens [37]. As an effective antimicrobial agent, the nanoemulsion could be an inhibition alternative for controlling *V. fluvialis* and *V. mimicus*, and particularly diseases spread in aquaculture.

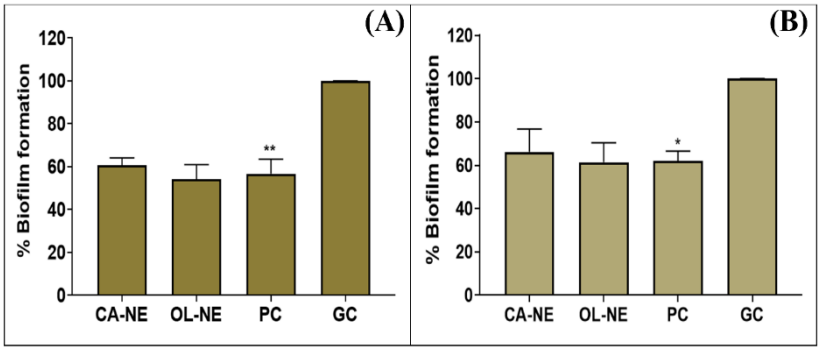

Figure 4. The experiment evaluated the percentage of biofilm formation of two commercially purchased *Spp. V. fluvialis and mimicus*. The **(A)** *V. fluvialis*; **(B)** *V. mimicus* were tested with castor and olive oils nanoemulsions, and successful inhibition was noted against both pathogens. CA-NE-Castor Oil-Nanoemulsion; OL-NE-Olive-Oil-Nanoemulsion; PC (Positive Control-Gentamicin); GC-growth control.

3.5. Live/dead staining analysis.

A live/dead assay was conducted to evaluate the viability of bacterial cells and explore the mechanism of action of tested nanoemulsions (NEs) and the antibiotic gentamicin. The results demonstrated that the tested compounds, including CA-NE, OL-NE, and gentamicin, exhibited a concentration-dependent effect (Sub-MIC), leading to increased bacterial cell death in Figure 5A-B. In Figure 5A, the percentages of dead cells of CA-NE and OL-NE are 41.71% and 44.31%, respectively, while gentamicin showed a 43.71% death rate against *V. fluvialis*. In contrast, the *V. mimicus*, the reported dead cell percentage, exhibited CA-NE (45.22%), OL-NE (54.72%), and the currently available antibiotics (54.87%) in Figure 5B. These findings indicate that the tested NEs (OL-NE with *V. fluvialis*) have the potential to be effective alternatives compared to conventional antimicrobial agents in various applications. The reduction in cell intensity caused by NEs was comparable to or even higher than the effect of current antibiotics [28]. Syto-9 is a fluorescent nucleic acid stain commonly used in live/dead assays to determine bacterial cell viability. When Syto-9 comes into contact with a bacterial cell with a compromised or damaged membrane, it can enter and interact with nucleic acids. This enables researchers to assess the viability of bacterial cells quantitatively and investigate

the effects of various compounds on bacterial cell survival, such as nanoemulsions or antibiotics [30, 29].

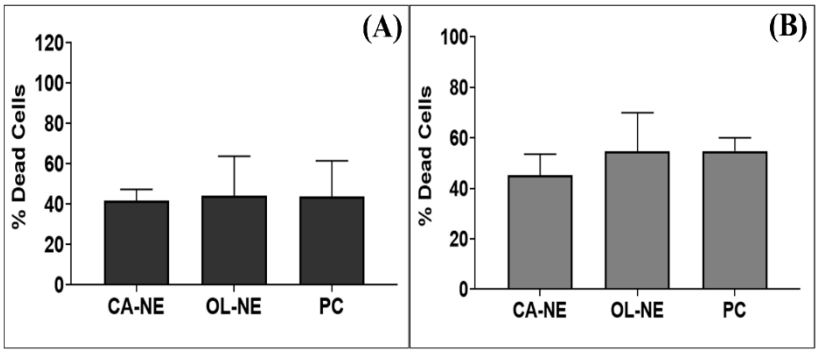

Figure5. (B)The Vibrios strains were treated with ozonated castor and olive oil nanoemulsions, including the antibiotic (Gentamicin). The graph represents the percentage of dead cells, testing with the potential nanoemulsions against *V. fluvialis* (**A**) and *V. mimicus* (**B**). CA-NE-Castor Oil-Nanoemulsion; OL-NE-Olive-Oil-Nanoemulsion; PC (positive control-Gentamicin).

3.6. Oxygen consumption rate in nanoemulsion.

According to research, gallic acid modulates ampicillin sensitivity against *Pseudomonas aeruginosa* [32]. An oxygen consumption rate study was performed to assess the effectuality of nanoemulsion on the bacterial cells by maintaining the young culture (4-6 hr) for treatment. The current antibiotic treatment concentration used (175 ug/ml), whereas NEs at (125 ug/ml). Significant fold reductions were noticed in respiration (OCR) with all two species compared to untreated cells (1.0-0 ug/ml). The NE treatment had a pronounced significant effect; each was applied directly through the fresh TS medium. The fold reduction for CA-NE was 0.67 fold, NE26 was 0.77 fold, and for antibiotics, 0.89-fold reduction. So, the better fold reduction of 0.22 (CA-NE) and 0.12 fold (OL-NE) than antibiotics against *V. fluvialis* (MTCC-4432) is shown in (Figure 6A). The increase in the nanomoles of oxygen/ml/min was recorded (Figure 6B). Meanwhile, CA-NE exhibited reductions of 0.53-fold, and OL-NE was 0.60-fold, whereas current antibiotics are 0.69-fold against *V. mimicus* (MTCC-4434) recorded. Therefore, CA-NE reduction signifies 0.16-fold better than OL-NE as 0.09-fold followed by antibiotics, as shown in (Figure 6C). The increase in the nanomoles of oxygen/ml/min was recorded against *V. mimicus*, shown in (Figure 6D). The antibiotic treatments inhibited the bacteria, indicating cellular respiration and metabolic activity suppression. It reflects the fold reductions, as it may suggest the inhibition of bacterial growth and survival [33,31]. Similarly, nanoemulsions are composed of nano-droplets of oil/water combination with a more lipophilic nature, stabilized by surfactants or co-surfactants and emulsifying agents [34,35,38]. NEs impact the bacterial cell membrane, potentially affecting cellular respiration and metabolic activity. A previous study suggested inhibited the growth of *B. subtilis*, *E. coli*, *P. aeruginosa*, and *S. aureus* [39,40]. This may occur due to cell membrane disruption, interference with membrane-bound enzymes or transport systems, or other mechanisms. As a result, bacterial cell death may experience reduced oxygen consumption, leading to an increased oxygen fold and inhibitory effects of nanoemulsions.

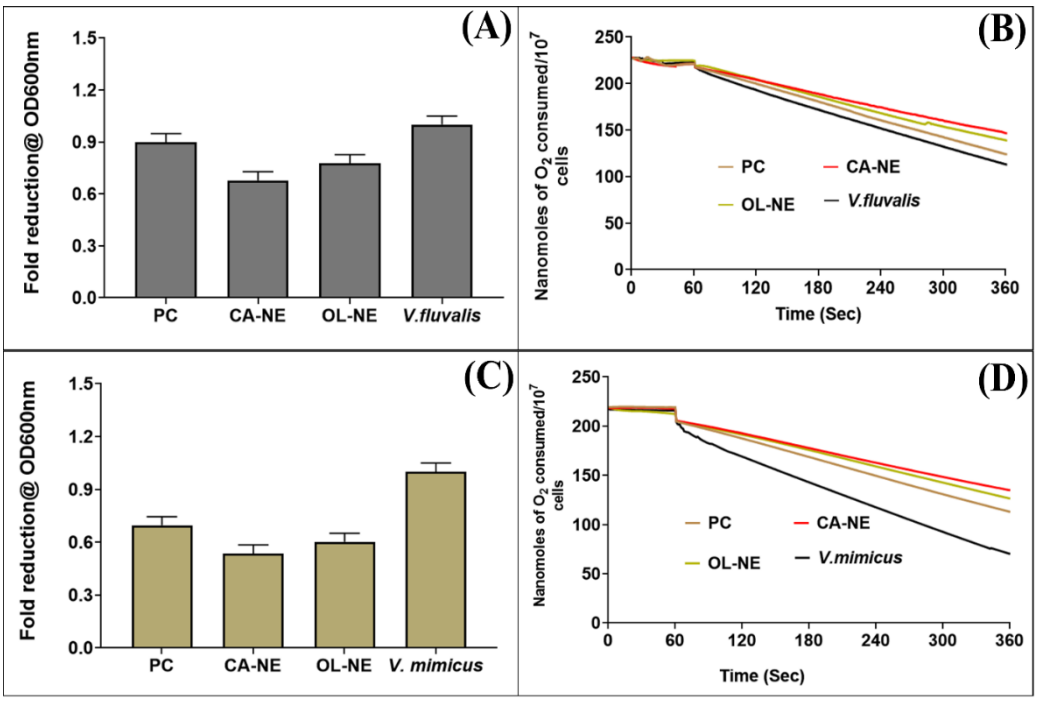

Figure 6. The results, depicted in a graph, show the overall effect of castor and olive oil NEs and antibiotics on the oxygen consumption rate (OCR) of all *V. fluvialis* and *V. mimicus*. **(A, C)** reduction in bacteria folds after treatment compared to untreated cells; **(B, D)** indicating the nanomoles O_2 consumed/second/milliliter of fresh media. The experiments were repeated three times, and the average values were plotted. The values are presented as means ± standard deviation (SD), with a sample size (n) of three independent experiments. PC-positive control; CA-NE-Castor Oil-Nanoemulsion; OL-NE-Olive-Oil-Nanoemulsion; OCR-oxygen consumption rate.

4. Conclusions

In conclusion, the results from the anti-adherence efficacy study of OL-NE demonstrated its superior performance compared to the antibiotic gentamicin. OL-NE exhibited a higher inhibition rate of 45.33% against *V. fluvialis*, while gentamicin only achieved a 29.27% inhibition rate. Furthermore, in the biofilm assay, OL-NE showed even greater inhibition with a rate of 45.89% against *V. fluvialis*, surpassing the efficacy of gentamicin. The live/dead staining results revealed that OL-NE caused a significant percentage of dead cells (54.72%) against *V. mimicus*, comparable to the effect of gentamicin (54.87%). Additionally, the oxygraph analysis provided valuable insights into the effectiveness of CA-NE. The oxygen consumption rate (OCR) reduction of CA-NE was measured at 0.67, indicating its better reduction rate (0.22-fold) against *V. fluvialis* than the current antibiotics, which exhibited a reduction rate of 0.89-fold compared with untreated (1.0) cells. These findings strongly suggest that nanoemulsions hold great promise as potential alternatives to traditional antibiotics in combating *V. fluvialis*, especially considering their better adherence prevention, biofilm inhibition, and OCR rate.

Furthermore, NEs also demonstrated noteworthy results in live/dead staining, particularly against *V. mimicus*. The results presented in this study highlight the potential of nanoemulsions as a new avenue for combating bacterial infections, offering an effective and promising alternative to currently available antibiotics. Further research and development in this area could lead to the formulation of innovative and efficient antibacterial treatments to address the growing concerns of antibiotic resistance.

Funding

This work was supported by the Indian Council of Medical Research (ICMR) [Project ID: 2020-4964].

Acknowledgments

The authors would like to thank B. S. Abdur Rahman Crescent Institute of Science and Technology for facilitating this study.

Conflicts of Interest

The authors declare no conflict of interest.

References

1. Mizuno, T.; Sultan, S.Z.; Kaneko, Y.; Yoshimura, T.; Maehara, Y.; Nakao, H.; Tsuchiya, T.; Shinoda, S.; Miyoshi, S.-i. Modulation of *Vibrio mimicus* hemolysin through limited proteolysis by an endogenous metalloprotease. *FEBS J.* **2009**, *276*, 825–834, https://doi.org/10.1111/j.1742-4658.2008.06827.x.
2. Miyoshi, S.-i.; Toko, N.; Dodo, T.; Nanko, A.; Mizuno, T. Second extracellular protease mediating maturation of *Vibrio mimicus* hemolysin. *World J. Microbiol. Biotechnol.* **2022**, *38*, 241, https://doi.org/10.1007/s11274-022-03436-9.
3. Kay, M.K.; Cartwright, E.J.; Maceachern, D.; McCullough, J.; Barzilay, E.; Mintz, E.; Duchin, J.S.; Macdonald, K.; Turnsek, M.; Tarr, C.; Talkington, D.; Newton, A.; Marfin, A.A. *Vibrio mimicus* Infection Associated with Crayfish Consumption, Spokane, Washington, 2010. *J. Food Prot.* **2012**, *75*, 762–764, https://doi.org/10.4315/0362-028X.JFP-11-410.
4. S, E.N.; Mothadaka, M.P. Vibrio mimicus and Its Antimicrobial Resistance in Fish and Aquatic Environments. In Handbook on Antimicrobial Resistance: Current Status, Trends in Detection and Mitigation Measures, Mothadaka, M.P., Vaiyapuri, M., Rao Badireddy, M., Nagarajrao Ravishankar, C., Bhatia, R., Jena, J., Eds.; Springer Nature Singapore, Singapore, **2023**; 1–21, https://doi.org/10.1007/978-981-16-9723-4_19-1.
5. Baffone, W.; Citterio, B.; Vittoria, E.; Casaroli, A.; Pianetti, A.; Campana, R.; Bruscolini, F. Determination of several potential virulence factors in *Vibrio* spp. isolated from sea water. *Food Microbiol.* **2001**, *18*, 479–488, https://doi.org/10.1006/fmic.2001.0441.
6. Fleischmann, S.; Herrig, I.; Wesp, J.; Stiedl, J.; Reifferscheid, G.; Strauch, E.; Alter, T.; Brennholt, N. Prevalence and Distribution of Potentially Human Pathogenic *Vibrio* spp. on German North and Baltic Sea Coasts. *Front. Cell. Infect. Microbiol.* **2022**, *12*, 846819, https://doi.org/10.3389/fcimb.2022.846819.
7. Singh, D.V.; Isac Sree, R.; Colwell, R.R. Development of a Hexaplex PCR Assay for Rapid Detection of Virulence and Regulatory Genes in *Vibrio cholerae* and *Vibrio mimicus*. *J. Clin. Microbiol.* **2002**, *40*, 4321–4324, https://doi.org/10.1128/JCM.40.11.4321-4324.2002.
8. Abioye, O.E.; Osunla, C.A.; Nontongana, N.; Okoh, A.I. Occurrence of virulence determinants in *vibrio cholerae*, *vibrio mimicus*, *vibrio alginolyticus*, and *vibrio parahaemolyticus* isolates from important water resources of Eastern Cape, South Africa. *BMC Microbiol.* **2023**, *23*, 316, https://doi.org/10.1186/s12866-023-03060-z.
9. Shinoda, S.; Nakagawa, T.; Shi, L.; Bi, K.; Kanoh, Y.; Tomochika, K.-i.; Miyoshi, S.-i.; Shimada, T. Distribution of Virulence-Associated Genes in Vibrio mimicus Isolates from Clinical and Environmental Origins. *Microbiol. Immunol.* **2004**, *48*, 547–551, https://doi.org/10.1111/j.1348-0421.2004.tb03551.x.
10. Hossain, M.; Ibne Momen, A.M.; Rahman, A.; Biswas, J.; Yasmin, M.; Nessa, J.; Ahsan, C.R. Draft-genome analysis provides insights into the virulence properties and genome plasticity of *Vibrio fluvialis* organisms isolated from shrimp farms and Turagriver in Bangladesh. *Arch. Microbiol.* **2022**, *204*, 527, https://doi.org/10.1007/s00203-022-03128-w.
11. Miyoshi, S.-I.; Ikehara, H.; Kumagai, M.; Mizuno, T.; Kawase, T.; Maehara, Y. Defensive Effects of Human Intestinal Antimicrobial Peptides against Infectious Diseases Caused by *Vibrio mimicus* and *V. vulnificus*. *Biocontrol Sci.* **2014**, *19*, 199–203, https://doi.org/10.4265/bio.19.199.

12. Boyd, E.F.; Moyer Kathryn, E.; Shi, L.; Waldor Matthew, K. Infectious CTXΦ and the Vibrio Pathogenicity Island Prophage in *Vibrio mimicus*: Evidence for Recent Horizontal Transfer between *V. mimicus* and *V. cholerae*. *Infect. Immun.* **2000**, *68*, 1507–1513, https://doi.org/10.1128/IAI.68.3.1507-1513.2000.
13. Wang, D.; Wang, H.; Zhou, Y.; Zhang, Q.; Zhang, F.; Du, P.; Wang, S.; Chen, C.; Kan, B. Genome Sequencing Reveals Unique Mutations in Characteristic Metabolic Pathways and the Transfer of Virulence Genes between *V. mimicus* and *V. cholerae*. *PLoS One* **2011**, *6*, e21299, https://doi.org/10.1371/journal.pone.0021299.
14. Huang, K.-C.; Wen-Wei Hsu, R. *Vibrio Fluvialis* Hemorrhagic Cellulitis and Cerebritis. *Clin. Infect. Dis.* **2005**, *40*, 75–77, https://doi.org/10.1086/429328.
15. John Albert, M.; Anowat Hossain, M.; Alam, K.; Kabir, I.; Neogi, P.K.B.; Tzipori, S. A fatal case associated with shigellosis and *Vibrio fluvialis* bacteremia. *Diagn. Microbiol. Infect. Dis.* **1991**, *14*, 509–510, https://doi.org/10.1016/0732-8893(91)90008-4.
16. Lee, J.Y.; Park, J.S.; Oh, S.H.; Kim, H.R.; Lee, J.N.; Shin, J.H. Acute infectious peritonitis caused by *Vibrio fluvialis*. *Diagn. Microbiol. Infect. Dis.* **2008**, *62*, 216–218, https://doi.org/10.1016/j.diagmicrobio.2008.05.012.
17. Chen, P.-J.; Tseng, C.-C.; Chan, H.-T.; Chao, C.-M. Acute Otitis Due to *Vibrio Fluvialis* after Swimming. *Case Rep. Emerg. Med*. **2012**, *2012*, 838904, https://doi.org/10.1155/2012/838904.
18. Hecht, J.; Borowiak, M.; Fortmeier, B.; Dikou, S.; Gierer, W.; Klempien, I.; Nekat, J.; Schaefer, S.; Strauch, E. Case Report: *Vibrio fluvialis* isolated from a wound infection after a piercing trauma in the Baltic Sea. *Access Microbiol.* **2022**, *4*, 000312, https://doi.org/10.1099/acmi.0.000312.
19. Bao, J.; Guo, D.; Jin, L.; Li, T.; Shi, H. Accurate Identification of Diverse N-acyl Homoserine Lactones in Marine *Vibrio fluvialis* by UHPLC-MS/MS. *Curr. Microbiol.* **2022**, *79*, 181, https://doi.org/10.1007/s00284-022-02879-5.
20. Liu, W.L.; Chiu, Y.H.; Chao, C.M.; Hou, C.C.; Lai, C.C. Biliary tract infection caused by *Vibrio fluvialis* in an immunocompromised patient. *Infection* **2011**, *39*, 495–496, https://doi.org/10.1007/s15010-011-0146-0.
21. Mushtaq, A.; Mohd Wani, S.; Malik, A.R.; Gull, A.; Ramniwas, S.; Ahmad Nayik, G.; Ercisli, S.; Alina Marc, R.; Ullah, R.; Bari, A. Recent insights into Nanoemulsions: Their preparation, properties and applications. *Food Chem. X* **2023**, *18*, 100684. https://doi.org/10.1016/j.fochx.2023.100684.
22. S, M.A.; Ahmed, J.; Ramalingam, K. The Essential Properties of Nanoemulsions: Basics of Nanoemulsion. In Handbook of Research on Nanoemulsion Applications in Agriculture, Food, Health, and Biomedical Sciences, Ramalingam, K., Ed.; IGI Global: Hershey, PA, USA, **2022**; 1–23, https://doi.org/10.4018/978-1-7998-8378-4.ch001.
23. Kim, G.W.; Yun, S.; Jang, J.; Lee, J.B.; Kim, S.Y. Enhanced stability, formulations, and rheological properties of nanoemulsions produced with microfludization for eco-friendly process. *J. Colloid Interface Sci.* **2023**, *646*, 311–319, https://doi.org/10.1016/j.jcis.2023.05.005.
24. Li, W.; Chen, H.; He, Z.; Han, C.; Liu, S.; Li, Y. Influence of surfactant and oil composition on the stability and antibacterial activity of eugenol nanoemulsions. *LWT - Food Sci. Technol.* **2015**, *62*, 39–47, https://doi.org/10.1016/j.lwt.2015.01.012.
25. S, R.; Parthasarathy, P.; P, R.; U, V.; S, H. Pungent anti-infective nanocolloids manipulate growth, biofilm formation, and CTX-M-15 gene expression in pathogens causing vibriosis. *Aquac. Int.* **2021**, *29*, 859–869, https://doi.org/10.1007/s10499-021-00660-2.
26. Zheng, H.; Huang, Y.; Liu, P.; Yan, L.; Zhou, Y.; Yang, C.; Wu, Y.; Qin, J.; Guo, Y.; Pei, X.; Guo, Y.; Cui, Y.; Liang, W. Population genomics of the food-borne pathogen *Vibrio fluvialis* reveals lineage associated pathogenicity-related genetic elements. *Microb. Genom.* **2022**, *8*, 000769 https://doi.org/10.1099/mgen.0.000769.
27. Tuan, L.C.; Khanh, N.V.; Tien, H.T.N.B.; Phuong, P.T.; Hieu, D.V.; Thanh, L.T.H.; Loc, N.H. The occurrence of antibiotic resistance *Vibrio* isolates from brackish water shrimp ponds in the coastal area in Thua Thien Hue, Vietnam. *J. Appl. Biol. Biotechnol.* **2023**, *11*, 123-128, https://doi.org/10.7324/JABB.2023.110211.
28. Vaou, N.; Stavropoulou, E.; Voidarou, C.; Tsigalou, C.; Bezirtzoglou, E. Towards Advances in Medicinal Plant Antimicrobial Activity: A Review Study on Challenges and Future Perspectives. *Microorganisms* **2021**, *9*, 2041, https://doi.org/10.3390/microorganisms9102041.
29. Robertson, J.; McGoverin, C.; Vanholsbeeck, F.; Swift, S. Optimisation of the Protocol for the LIVE/DEAD® BacLight™ Bacterial Viability Kit for Rapid Determination of Bacterial Load. *Front. Microbiol.* **2019**, *10*, 801, https://doi.org/10.3389/fmicb.2019.00801.

30. McGoverin, C.; Robertson, J.; Jonmohamadi, Y.; Swift, S.; Vanholsbeeck, F. Species Dependence of SYTO 9 Staining of Bacteria. *Front. Microbiol.* **2020**, *11*, 545419, https://doi.org/10.3389/fmicb.2020.545419.
31. Keller, M.; Han, X.; Dörr, T. Disrupting Central Carbon Metabolism Increases β-Lactam Antibiotic Susceptibility in *Vibrio cholerae*. *J. Bacteriol.* **2023**, *205*, e00476-00422, https://doi.org/10.1128/jb.00476-22.
32. Kosuru, R.Y.; Aashique, M.; Fathima, A.; Roy, A.; Bera, S. Revealing the Dual Role of Gallic Acid in Modulating Ampicillin Sensitivity of *Pseudomonas Aeruginosa* Biofilms. *Future Microbiol.* **2018**, *13*, 297–312, https://doi.org/10.2217/fmb-2017-0132.
33. Lopatkin, A.J.; Stokes, J.M.; Zheng, E.J.; Yang, J.H.; Takahashi, M.K.; You, L.; Collins, J.J. Bacterial metabolic state more accurately predicts antibiotic lethality than growth rate. *Nat. Microbiol.* **2019**, *4*, 2109–2117, https://doi.org/10.1038/s41564-019-0536-0.
34. Shaker, D.S.; Ishak, R.A.H.; Ghoneim, A.; Elhuoni, M.A. Nanoemulsion: A Review on Mechanisms for the Transdermal Delivery of Hydrophobic and Hydrophilic Drugs. *Sci. Pharm.* **2019**, *87*, 17, https://doi.org/10.3390/scipharm87030017.
35. Keykhasalar, R.; Homayouni Tabrizi, M.; Ardalan, P. Antioxidant Property and Bactericidal Activity of *Linum Usitatissimum* Seed Essential Oil Nanoemulsion (LSEO-NE) on *Staphylococcus Aureus*. *Int. J. Infect.* **2020**, *7*, e101639, https://doi.org/10.5812/iji.101639.
36. Xiao, Y.; Huang, Z.; Yu, K.; Wang, M.; Gao, H.; Bai, X.; Jiang, M.; Wang, D. Distribution and Molecular Characteristics of *Vibrio* Species Isolated from Aquatic Environments in China, 2020. *Microorganisms* **2022**, *10*, 2007, https://doi.org/10.3390/microorganisms10102007.
37. Khan, M.H.; Ramalingam, K. Synthesis of antimicrobial nanoemulsions and its effectuality for the treatment of multi-drug resistant ESKAPE pathogens. *Biocatal. Agric. Biotechnol.* **2019**, *18*, 101025, https://doi.org/10.1016/j.bcab.2019.101025.
38. Sarfraz, H.; Ahmad, I.Z. A systematic review on the pharmacological potential of *Linum usitatissimum* L.: a significant nutraceutical plant. *J. Herb. Med.* **2023**, *42*, 100755, https://doi.org/10.1016/j.hermed.2023.100755.
39. Nasra, S.; Meghani, N.; Kumar, A. Nanoemulsion-Based System as a Novel and Promising Approach for Enhancing the Antimicrobial and Antitumoral Activity of *Thymus Vulgaris* (L.) Oil in Human Hepatocellular Carcinoma Cells. *Appl. Biochem. Biotechnol.* **2024**, *196*, 949-970, https://doi.org/10.1007/s12010-023-04571-1.
40. Juneja, M.; Suthar, T.; Pardhi, V.P.; Ahmad, J.; Jain, K. Emerging Trends and Promises of Nanoemulsions in Therapeutics of Infectious Diseases. *Nanomedicine* **2022**, *17*, 793–812, https://doi.org/10.2217/nnm-2022-0006.